Regulation of Gating and Rundown of HCN Hyperpolarization-activated Channels by Exogenous and Endogenous PIP_2

Phillip Pian,[1] Annalisa Bucchi,[2] Richard B. Robinson,[2,3] and Steven A. Siegelbaum[1,2,4]

[1]Center for Neurobiology and Behavior, [2]Department of Pharmacology, [3]Center for Molecular Therapeutics, and [4]Howard Hughes Medical Institute, Columbia University Medical Center, New York, NY 10032

The voltage dependence of activation of the HCN hyperpolarization-activated cation channels is shifted in inside-out patches by −40 to −60 mV relative to activation in intact cells, a phenomenon referred to as rundown. Less than 20 mV of this hyperpolarizing shift can be due to the influence of the canonical modulator of HCN channels, cAMP. Here we study the role of phosphatidylinositol 4,5-bisphosphate ($PI(4,5)P_2$) in HCN channel rundown, as hydrolysis of $PI(4,5)P_2$ by lipid phosphatases is thought to underlie rundown of several other channels. We find that bath application of exogenous $PI(4,5)P_2$ reverses the effect of rundown, producing a large depolarizing shift in HCN2 activation. A synthetic short chain analogue of $PI(4,5)P_2$, dioctanoyl phosphatidylinositol 4,5-bisphosphate, shifts the HCN2 activation curve to more positive potentials in a dose-dependent manner. Other dioctanoyl phosphatidylinositides with one or more phosphates on the lipid headgroup also shift activation, although phosphatidylinositol (PI) is ineffective. Several lines of evidence suggest that HCN2 is also regulated by endogenous $PI(4,5)P_2$: (a) blockade of phosphatases slows the hyperpolarizing shift upon patch excision; (b) application of an antibody that binds and depletes membrane PIP_2 causes a further hyperpolarizing shift in activation; (c) the shift in activation upon patch excision can be partially reversed by MgATP; and (d) the effect of MgATP is blocked by wortmannin, an inhibitor of PI kinases. Finally, recordings from rabbit sinoatrial cells demonstrate that diC_8 $PI(4,5)P_2$ delays the rundown of native HCN currents. Thus, both native and recombinant HCN channels are regulated by $PI(4,5)P_2$.

The Journal of General Physiology

INTRODUCTION

The HCN channel gene family (HCN1–4) encodes the hyperpolarization-activated cation channels that generate the excitatory pacemaker current (I_h or I_f), which contributes to the rhythmic activity of both neurons and cardiac myocytes (Robinson and Siegelbaum, 2003; DiFrancesco, 2006). Cyclic AMP has long been known to directly enhance I_h by shifting its activation to more positive potentials (DiFrancesco and Tortora, 1991). More recently, HCN channel function has been found to be regulated by several other mechanisms, including tyrosine phosphorylation (Yu et al., 2004; Zong et al., 2005; Arinsburg et al., 2006); association with MiRP1, a potential HCN channel β subunit (Yu et al., 2001); and association with TRIP8b, a cytoplasmic protein that controls channel trafficking (Santoro et al., 2004). Despite the discovery of these new modes of I_h regulation, several lines of evidence, including the phenomenon of channel rundown, suggest the existence of other regulatory mechanisms that have yet to be identified.

The activation of I_h shifts by as much as −40 to −60 mV relative to that in intact cells during recordings from inside-out patches or during prolonged dialysis associated with whole-cell recordings, for both native HCN channels in cardiac myocytes (DiFrancesco et al., 1986; DiFrancesco and Tortora, 1991; DiFrancesco and Mangoni, 1994; Bois et al., 1997) and recombinant channels in heterologous cells (Chen et al., 2001). In contrast, this rundown phenomenon is not observed in perforated-patch whole-cell recordings, suggesting that rundown may be due to the loss of intracellular constituents that regulate I_h in intact cells (Zhou and Lipsius, 1993). Since cAMP produces, at most, a 20-mV positive shift in the activation of I_h, loss of a modulatory influence of cyclic nucleotides after patch excision can account for no more than half of the 40–60-mV shift seen during rundown (DiFrancesco and Tortora, 1991; Chen et al., 2001), suggesting the presence of other modulatory factors. Neither MiRP1 (Yu et al., 2001) nor TRIP8b (Santoro et al., 2004) are likely candidates for this factor since these proteins do not act to shift HCN activation gating to more positive potentials in intact cells. Although overexpression of Src tyrosine kinase in HEK-293 cells does shift the voltage dependence of HCN channel activation to more positive

Correspondence to Steven A. Siegelbaum: sas8@columbia.edu

The online version of this article contains supplemental material.

Abbreviations used in this paper: HCN, hyperpolarization-activated, cyclic nucleotide-regulated, cation-nonselective; $PI(4,5)P_2$ or PIP_2, phosphatidylinositol 4,5-bisphosphate; diC_8, dioctanoyl; PI, phosphatidylinositol; LC acyl-coA, long chain acyl-coenzyme A; K_{ATP}, ATP-sensitive K^+; K_{in}, inwardly rectifying K^+.

potentials (Arinsburg et al., 2006), loss of Src activity is also unlikely to underlie rundown because pharmacological inhibition of endogenous Src has relatively little effect on the voltage dependence of HCN channel activation in intact cells (Zong et al., 2005; Arinsburg et al., 2006). Thus, the identity of the regulatory mechanism responsible for the rundown of I_h activation remains unclear.

Interestingly, rundown may be of physiological relevance since a −40-mV hyperpolarizing shift in HCN channel activation is observed in intact ventricular myocytes during postnatal development (Robinson et al., 1997) and this shift does not appear to be due to changes in basal cAMP concentration (Qu et al., 2001). Moreover, during heart failure, HCN channel activation in ventricular myocytes shifts back toward more positive potentials, producing a proarrhythmic increase in pacemaker current (Cerbai et al., 1997).

One promising candidate molecule for underlying rundown is the membrane phospholipid, phosphatidylinositol 4,5-bisphosphate ($PI(4,5)P_2$). Although $PI(4,5)P_2$ was initially discovered as a precursor for two other second messengers, inositol trisphosphate and diacylglycerol, it has more recently been shown to play an active role in cellular physiology, including enzyme activation, membrane trafficking, and, more specifically, the regulation of ion channels (Hilgemann et al., 2001; McLaughlin et al., 2002; Suh and Hille, 2005). Here we examine the hypothesis that the hyperpolarizing shift in HCN channel gating upon patch excision results from the loss of a basal regulatory action of $PI(4,5)P_2$ during rundown due to lipid dephosphorylation by membrane-bound phosphatases. Such a mechanism has been previously found to underlie the functional changes observed upon patch excision for a variety of other ion channels, including inward rectifying K^+ channels (Zhang et al., 1999) and P/Q-type voltage-gated Ca^{2+} channels (Wu et al., 2002; Suh and Hille, 2005).

To address this hypothesis, we examined both recombinant HCN2 channels expressed in *Xenopus* oocytes and native HCN currents in cardiac sinoatrial cells. We employed several techniques to manipulate membrane levels of $PI(4,5)P_2$ in both excised patches and whole oocytes, while monitoring the consequences on HCN2 gating. The results from these experiments are consistent with the idea that HCN2 and native sinoatrial HCN currents are regulated by both exogenous and endogenous $PI(4,5)P_2$.

MATERIALS AND METHODS

Expression in *Xenopus* Oocytes

Mouse HCN2 was previously cloned into pGEMHE (Chen et al., 2001) and the HCN2/FPN mutant was previously constructed (Zhou et al., 2004). PIP5K (phosphatidylinositol-4-phosphate 5-kinase) in the pGEMHE vector was the generous gift of the Logothetis laboratory. pGEMHE:HCN2 and pGEMHE:PIP5K were linearized by SphI and HpaI, respectively. cRNA was transcribed from linearized DNA using T7 RNA polymerase (mMessage mMachine; Ambion) and injected into *Xenopus* oocytes as described previously (Goulding et al., 1992). Oocytes were injected with 5 ng HCN2 cRNA; in coexpression experiments, oocytes were injected with 20 ng HCN2 and 20 ng PIP5K cRNA.

Xenopus Oocyte Electrophysiological Recordings

Cell-free inside-out patches were obtained 5–6 d after cRNA injection, and data were acquired using a patch-clamp amplifier (Axopatch 200B; Axon Instruments, Inc.). Patch pipettes had resistances of 1–3 MΩ and were filled with a pipette solution containing (in mM) 96 KCl, 1 NaCl, 10 HEPES, 1.8 $CaCl_2$, and 1 $MgCl_2$, pH 7.4. The bath solution contained 96 KCl, 1 NaCl, 10 HEPES, and 5 EGTA, pH 7.4. The FV bath solution used to inhibit phosphatases contained 96 KCl, 0.4 NaCl, 10 HEPES, 5 EGTA, 0.1 KF, 0.2 Na_3VO_4, pH 7.4. An Ag-AgCl ground wire was connected to the bath solution by a 3 M KCl agar bridge electrode, and junction potential was compensated before the formation of each patch. Linear leak current was not subtracted. Data were filtered at 1 kHz with an 8-pole low-pass Bessel filter (Frequency Devices) and sampled at 2 kHz with an ITC-16 interface (Instrutech) and Pulse software (HEKA).

Two microelectrode voltage-clamp recordings were obtained 1 d after cRNA injection using an oocyte clamp amplifier (model OC-725C; Warner Instruments). Data were filtered at 1 kHz and sampled at 2 kHz. The recordings were obtained with the oocytes bathed in an extracellular solution containing (in mM) 96 KCl, 2 NaCl, 10 HEPES, and 2 $MgCl_2$, pH 7.5. Microelectrodes were filled with 3 M KCl and had resistances of 0.5–2 MΩ.

Hyperpolarizing voltages in 10-mV step increments were applied to either inside-out patches or intact oocytes from a holding potential of −30 mV. All recordings were obtained at room temperature (18–22°C).

Data Analysis

HCN currents were analyzed as previously described (Chen et al., 2001). Activation curves were determined from plots of tail current amplitude (measured at −40 mV) as a function of test voltage during 3-s hyperpolarizing steps. Activation curves were fit with a Boltzmann equation to obtain the midpoint voltage of activation ($V_{1/2}$) and slope factor (s) of the relation (both in units of mV). Dose–response curves plotting the magnitude of the shift in $V_{1/2}$ as a function of diC_8 $PI(4,5)P_2$ concentration were measured and fitted with the Hill equation to obtain the maximal shift in $V_{1/2}$ at saturating lipid concentration, the concentration of lipid producing a half-maximal shift ($K_{1/2}$), and the Hill coefficient (h). Analysis was done using PulseFit (HEKA), Excel (Microsoft), and Origin (Microcal). Single comparisons between two experimental conditions were evaluated by a Student's *t* test. Comparisons involving multiple populations were evaluated by ANOVA with a Scheffe Post-Hoc test.

Experiments on Rabbit Sinoatrial Cells

Animal protocols conformed to the guidelines for the care and use of laboratory animals (National Institutes of Health publication no. 85–23). Rabbit sinoatrial cells were isolated as reported (DiFrancesco et al., 1986). Whole-cell patch-clamp experiments were performed using pipettes with a resistance of 2.5–4 MΩ filled with a solution containing (in mM) 130 aspartic acid, 146 KOH, 10 NaCl, 2 $CaCl_2$, 5 EGTA-KOH, 2 Mg-ATP, and 10 HEPES-KOH, pH 7.2. Cells were superfused with an extracellular solution containing 140 NaCl, 2.3 NaOH, 1 $MgCl_2$, 5.4 KCl, 1.8 $CaCl_2$, 5 HEPES, 10 glucose, 2 $MnCl_2$, and 1 $BaCl_2$, pH 7.4. Currents were recorded and filtered on-line at 1 kHz with an Axopatch 200B amplifier, and acquired using pClamp 9.0 software (Axon Instruments, Inc.). Recordings were performed at 32°C.

Activation curves were measured using a two-step protocol in which voltage steps from −25 to −115 or −145 mV were applied from a holding potential of −35 mV, followed by a step to −70 mV. To allow HCN channels to reach steady-state activation at all voltages, the duration of test steps varied from 10 s at −25 mV to 5 s at −145 mV while the duration of the step to −70 mV increased from 8 to 13.5 s after steps from more hyperpolarized voltages. The normalized plot of tail current versus test voltage was fitted with a Boltzmann function to obtain the $V_{1/2}$ and slope factor. Values are given as the mean ± SEM and data were compared using Student's *t* test for single comparisons and two-way ANOVA followed by a Bonferroni Post-Hoc test for multiple comparisons. Values of $P < 0.05$ were considered significant.

Reagents and Drugs

An aqueous stock solution of 0.5 mM native $PI(4,5)P_2$ (Calbiochem) was sonicated and aliquoted before snap freezing in liquid nitrogen. Aliquots were stored at −80°C until the day of the experiment, when working solutions were sonicated a second time. Dioctanoyl (diC_8) forms of PI, PI(4)P, $PI(3,4)P_2$, $PI(4,5)P_2$, and $PI(3,4,5)P_3$ (Echelon) were dissolved in water to make 2.5 mM stock solutions and stored in aliquots at −80°C. Oleoyl CoA (Sigma-Aldrich) was dissolved in water at a concentration of 5 mM. Anti-PIP_2 mAb and anti-hGM-CSF Ab (Assay Designs) were stored at −20°C at a concentration of 0.909 μg/μl. Antibodies were diluted 1:30 with bath solution to make working solutions. Heat-inactivated anti-PIP_2 mAb was prepared using a 90-min incubation in a 95°C water bath. Wortmannin (Sigma-Aldrich) was dissolved in DMSO at a concentration of 30 mM and stored in aliquots at −20°C. LY294002 (Biomol) was dissolved in DMSO at a concentration of 50 mM and stored in aliquots at −20°C. Poly-D-lysine HBr with a molecular weight of 1–4 kD was applied to patches at a final concentration of 25 μg/ml. Materials were purchased from Sigma-Aldrich unless otherwise noted.

Online Supplemental Material

Additional experimental data (available online at http://www.jgp.org/cgi/content/full/jgp.200609648/DC1) show the effect of rundown on the $V_{1/2}$ of HCN2 (Fig. S1) and the effect of phosphatidylinositides on maximal tail current amplitude (Fig. S2).

RESULTS

Exogenous Phosphatidylinositol Phosphates Alter the Voltage-dependent Gating of HCN2 Channels

Hyperpolarization-activated currents were elicited by a series of 3-s hyperpolarizing test pulses in membrane patches from *Xenopus* oocytes expressing HCN2. The midpoint voltage of activation from tail current activation curves ($V_{1/2}$) was approximately −80 mV when recorded in cell-attached patches before patch excision or from intact oocytes using two-microelectrode voltage clamp (Chen et al., 2001). However, within 1 min of formation of an inside-out patch, the $V_{1/2}$ had shifted by −40 mV, to approximately −120 mV. The $V_{1/2}$ was then stable over the next 10 min, indicating that this rundown in the voltage dependence of activation rapidly reached completion (Fig. S1, available at http://www.jgp.org/cgi/content/full/jgp.200609648/DC1).

The role of $PI(4,5)P_2$ in HCN channel gating was first studied by application of exogenous $PI(4,5)P_2$ to inside-out patches after rundown was complete. Bath application of 1 μM $PI(4,5)P_2$ isolated from native tissues, which consists predominantly of phosphatidylinositol 4,5-bisphosphate with an arachidonyl acyl chain in position 2 and a stearyl acyl chain at position 3 (AASt) (Rohacs et al., 2002), produced a large, gradual positive shift in the voltage dependence of HCN2 activation (Fig. 1, A and C). The time course of the shift in $V_{1/2}$ upon application of $PI(4,5)P_2$ was fit by a single exponential function with a $t_{1/2}$ value (time to produce a half maximal effect) of ∼250 s. The average shift in $V_{1/2}$ after 28 min of exposure to phospholipid was +31.8 ± 5.1 mV ($n = 4$; see Fig. 3 B).

Given the slow rate at which native $PI(4,5)P_2$ altered the voltage-dependent activation of HCN2, we next examined the short-acyl chain analogue of $PI(4,5)P_2$, dioctanoyl phosphatidylinositol 4,5-bisphosphate (diC_8 $PI(4,5)P_2$), since this analogue has been reported to act more rapidly than long chain lipids (Rohacs et al., 2002). Application of 25 μM diC_8 $PI(4,5)P_2$ caused a significant positive shift in the activation curve of HCN2, which occurred more quickly but was smaller in magnitude than the shift caused by 1 μM AASt $PI(4,5)P_2$ (Fig. 1, B and D). The onset of the shift in $V_{1/2}$ with diC_8 $PI(4,5)P_2$ ($n = 10$) had a $t_{1/2}$ value of 86 s, three times faster than the effect of full-length $PI(4,5)P_2$ (the increased rate of action of diC_8 $PI(4,5)P_2$ may reflect the fact that it needed to be applied at a higher concentration than the more potent full-length AASt $PI(4,5)P_2$). The average shift in $V_{1/2}$ of HCN2 after 10 min exposure to 25 μM diC_8 $PI(4,5)P_2$ was +15.4 ± 0.8 mV ($n = 12$; see Fig. 3 B), and there was a dose-dependent relation between the shift in $V_{1/2}$ and the concentration of diC_8 $PI(4,5)P_2$ (Fig. 2 A). A fit of the Hill equation to the dose–response curve yielded a value for the maximal shift in $V_{1/2}$ of +20.9 mV, a $K_{1/2}$ value of 10.9 μM, and a Hill coefficient (h) of 1.11.

Both full-length $PI(4,5)P_2$ and diC_8 $PI(4,5)P_2$ had a variable effect on the peak tail current amplitude after steps to negative voltages where voltage-dependent activation was complete (see Fig. S2). On average, there was a small decrease in peak current amplitude with both 25 μM full-length $PI(4,5)P_2$ (37.1% ± 18.7% decrease; range of 0.7% increase to 88.0% decrease; $n = 4$) and 25 μM diC_8 $PI(4,5)P_2$ (36.2% ± 6.8% decrease; range of 6.8% increase to 73.3% decrease; $n = 12$). However, these changes were not statistically significant when the effects of $PI(4,5)P_2$ were analyzed over an entire dose–response curve, including control experiments without $PI(4,5)P_2$ application (13.1 ± 1.6% decrease; $n = 3$; $P > 0.35$; ANOVA).

We next examined the effects of diC_8 $PI(4,5)P_2$ on the activation and deactivation kinetics of HCN2 channels (Fig. 2 B). Currents during hyperpolarizing voltage steps were fit with a single exponential to determine an effective time constant of activation. There was no significant effect of $PI(4,5)P_2$ on the time constant of

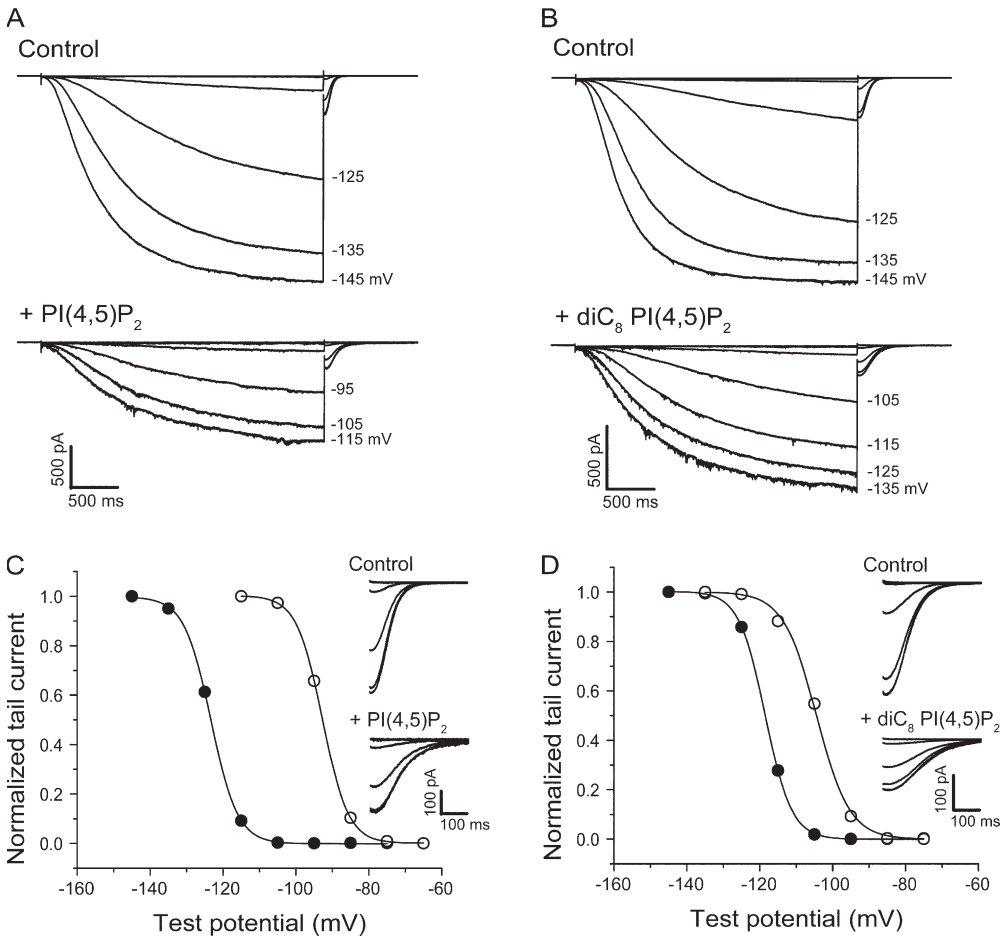

Figure 1. Phosphatidylinositol 4,5-bisphosphate ($PI(4,5)P_2$) and dioctanoyl phosphatidylinositol 4,5-bisphosphate (diC_8 $PI(4,5)P_2$) cause depolarizing shifts in the activation of HCN2. Macroscopic HCN2 currents are shown for individual inside-out patches in response to a series of hyperpolarizing voltage steps. (A) Before (top) and after (bottom) a 15' bath application of 1 μM native $PI(4,5)P_2$. (B) Before (top) and after (bottom) a 10' bath application of 25 μM diC_8 $PI(4,5)P_2$. (C and D) Normalized tail currents from A and B, respectively, plotted as a function of test potential and fit with the Boltzmann equation. Data obtained in absence (filled circles) or presence (open circles) of $PI(4,5)P_2$ and diC_8 $PI(4,5)P_2$ application. Insets show expanded records of tail currents from A and B, measured at −40 mV.

activation with steps to −115 or −125 mV. However, we observed a significant slowing of activation with steps to −135 mV ($P < 0.02$; *t* test). We also observed a significant twofold slowing in the rate of channel deactivation, measured by the time constant of tail current decay upon return of the membrane to −40 mV ($P < 0.001$; *t* test).

Specificity Profile of HCN2 for Dioctanoyl Phosphatidylinositol Phosphates

Different $PI(4,5)P_2$ binding domains and $PI(4,5)P_2$-regulated ion channels show varying degrees of specificity for $PI(4,5)P_2$ versus phosphatidylinositides that contain different numbers and positions of phosphates on the inositol headgroup (Rohacs et al., 1999; McLaughlin et al., 2002). To determine the lipid specificity profile for HCN2, we compared the actions of a variety of PI lipids, all applied at the same concentration (25 μM) (Fig. 3 A).

Application of dioctanoyl phosphatidylinositol (diC_8 PI), whose inositol headgroup is nonphosphorylated, produced no voltage shift in the HCN2 activation curve (−0.3 ± 1.7 mV, $n = 3$), indicating the need for one or more phosphate moieties (or alternatively, a requirement for a larger headgroup). A phosphoinositide with a single phosphate, dioctanoyl phosphatidylinositol 4-phosphate (diC_8 PI(4)P), produced a small 7.5 ± 2.0 mV ($n = 6$) positive shift in the $V_{1/2}$ that was significantly less than the 15.4-mV shift seen with 25 μM diC_8 $PI(4,5)P_2$ ($P < 0.02$; ANOVA). Application of a bisphosphate isomer distinct from $PI(4,5)P_2$, dioctanoyl phosphatidylinositol 3,4-bisphosphate (diC_8 $PI(3,4)P_2$), caused a 12.3 ± 1.8-mV depolarizing shift ($n = 7$), whereas dioctanoyl phosphatidylinositol 3,4,5-trisphosphate (diC_8 $PI(3,4,5)P_3$) produced a 9.3 ± 1.8-mV depolarizing shift ($n = 8$). Although these responses to diC_8 $PI(3,4)P_2$ and diC_8 $PI(3,4,5)P_3$ were somewhat smaller than the response to diC_8 $PI(4,5)P_2$, the differences were not statistically significant. Thus HCN2 is relatively nonselective among the polyphosphoinositides, although the inositol sugar of PI may need to be phosphorylated for modulation to occur.

ATP-sensitive K^+ channels (K_{ATP}) are the least specific of the inwardly rectifying K^+ channels in their activation by phosphoinositides and are uniquely activated by long chain (LC) acyl-CoA, an effect that is thought to reflect this lack of specificity (Rohacs et al., 2003). Given the low phosphoinositide specificity of HCN2, we tested the ability of LC acyl-CoA to alter its gating. Bath application of 1 μM Oleoyl CoA caused a +16.0 ± 1.7-mV

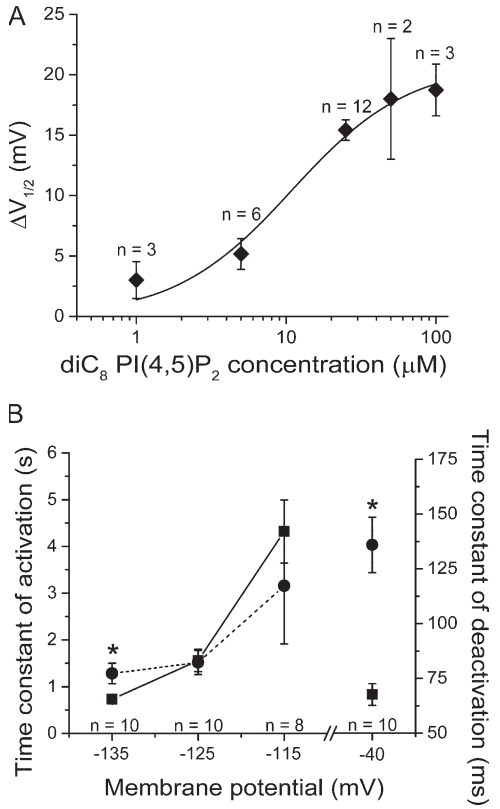

Figure 2. Action of diC_8 $PI(4,5)P_2$ on the gating of HCN2. (A) Dose–response curve for shift in $V_{1/2}$ ($\Delta V_{1/2}$) as a function of concentration of diC_8 $PI(4,5)P_2$. Data fit with the Hill equation. (B) Time constants (τ) of HCN2 current activation (left) and deactivation (right) in absence (squares, solid line) and presence (circles, dashed line) of 25 μM diC_8 $PI(4,5)P_2$. The difference between the time constants of activation at −135 mV before (0.731 ± 0.079 s) and after (1.28 ± 0.22 s) diC_8 $PI(4,5)P_2$ application were statistically significant (*, $P < 0.02$, *t* test). The difference between the time constants of deactivation at −40 mV before (67.6 ± 5.0 ms) and after (136 ± 13 ms) diC_8 $PI(4,5)P_2$ application were also statistically significant (*, $P < 0.001$, *t* test).

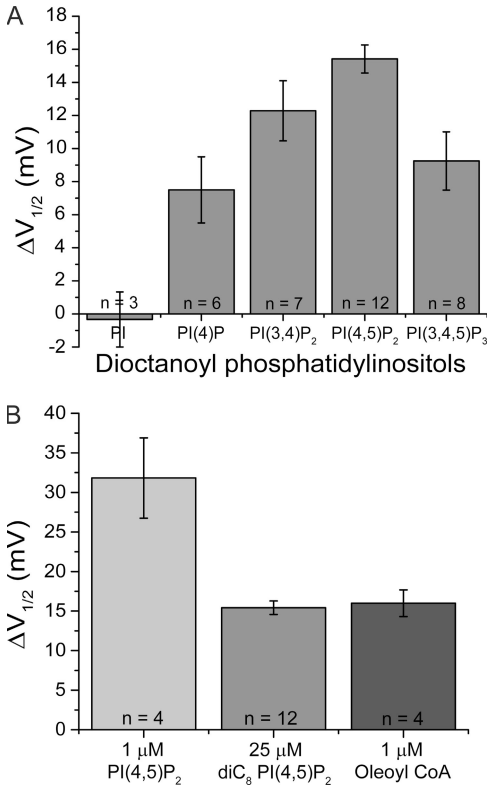

Figure 3. Shift in $V_{1/2}$ of HCN2 depends on number and location of inositol phosphates and on acyl chain length. (A) $V_{1/2}$ shifts with 10-min applications of dioctanoyl phosphatidylinositol (PI) (−0.3 ± 1.7 mV, $n = 3$), dioctanoyl phosphatidylinositol 4-phosphate (PI(4)P) (+7.5 ± 2.0 mV, $n = 6$), dioctanoyl phosphatidylinositol 3,4-bisphosphate ($PI(3,4)P_2$) (+12.3 ± 1.8 mV, $n = 7$), dioctanoyl phosphatidylinositol 4,5-bisphosphate ($PI(4,5)P_2$), and dioctanoyl phosphatidylinositol 3,4,5-trisphosphate ($PI(3,4,5)P_3$) (+9.3 ± 1.8 mV, $n = 8$). Differences between the responses to diC_8 $PI(4,5)P_2$ and diC_8 $PI(3,4,5)P_3$ and between the responses to diC_8 $PI(4,5)P_2$ and diC_8 PI(4)P are statistically significant ($P < 0.05$; ANOVA, Post Hoc). (B) $V_{1/2}$ shifts after 28-min application of 1 μM of native $PI(4,5)P_2$ (+31.8 ± 5.1 mV, $n = 4$), 10-min application of 25 μM diC_8 $PI(4,5)P_2$ (+15.4 ± 0.8 mV, $n = 12$), and 2-min application of 1 μM oleoyl coA (+16.0 ± 1.7 mV, $n = 4$).

shift ($n = 4$) in the HCN2 activation curve that was complete within 2 min. The magnitude of this effect was similar to the shift seen with 25 μM diC_8 $PI(4,5)P_2$ but significantly smaller than the shift seen with 1 μM native $PI(4,5)P_2$ (Fig. 3 B). Thus, HCN2 and K_{ATP} appear to define a class of channels that respond to LC acyl-CoA and exhibit a low phosphoinositide selectivity. It is interesting to note that fatty acyl-CoA is a major metabolite of cardiac myocytes, suggesting a possible physiological or pathophysiological role of this modulation.

Interaction of diC_8 $PI(4,5)P_2$ and cAMP

Because the effect of $PI(4,5)P_2$ to shift the activation of HCN2 to positive voltages is qualitatively similar to the modulatory action of cAMP, we explored the possibility that these two compounds act through similar mechanisms by determining whether cAMP application could occlude the response to diC_8 $PI(4,5)P_2$ (Fig. 4). Inside-out patches were initially exposed to a saturating concentration of cAMP (10 μM), which resulted in a +15.5 ± 0.6-mV shift in the $V_{1/2}$ ($n = 4$). The subsequent addition of 25 μM diC_8 $PI(4,5)P_2$ in the continued presence of 10 μM cAMP produced a further shift of +9.5 ± 0.7 mV ($n = 4$), resulting in a cumulative shift in $V_{1/2}$ of +25.0 ± 0.7 mV (Fig. 4 A). Thus, application of a saturating concentration of cAMP did not completely block the effect of diC_8 $PI(4,5)P_2$. Nonetheless, the effect of the lipid in the presence of cAMP was significantly less than the 15.4-mV shift in the absence of cAMP ($P < 0.01$; *t* test). This suggests that the two compounds bind to distinct sites but may recruit a convergent biophysical mechanism to alter the gating of HCN channels.

An interaction between cAMP and diC_8 $PI(4,5)P_2$ was also seen in their effects on the kinetics of HCN2 tail

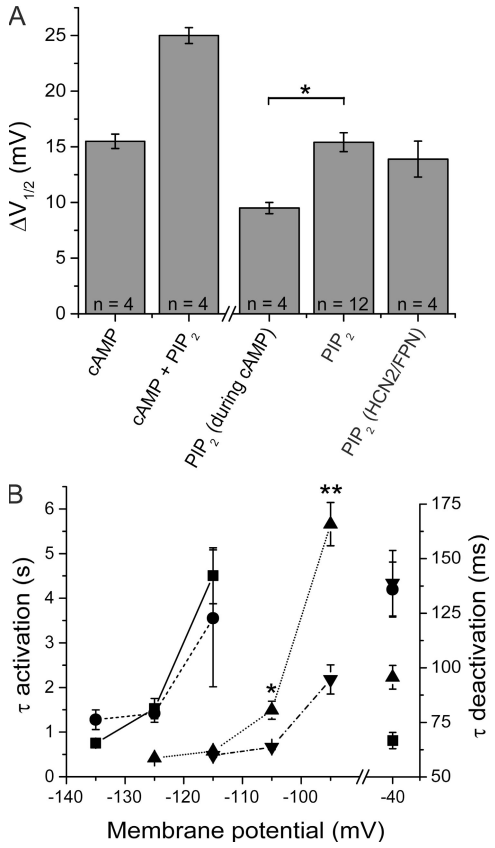

Figure 4. Effects of cAMP and diC_8 $PI(4,5)P_2$ on $V_{1/2}$ and channel kinetics are not independent. (A) Interaction of effects of cAMP and diC_8 $PI(4,5)P_2$ on $V_{1/2}$. Bars show the following (from left to right): cAMP, shift in $V_{1/2}$ in response to 10 μM cAMP; cAMP + PIP_2, shift in $V_{1/2}$ in response to 10 μM cAMP plus 25 μM diC_8 $PI(4,5)P_2$; PIP_2 (during cAMP), the difference between the shift in $V_{1/2}$ in response to cAMP plus diC_8 $PI(4,5)P_2$ and the shift produced by cAMP alone; PIP_2, shift in response to 25 μM diC_8 $PI(4,5)P_2$ alone; PIP_2 (HCN2/FPN), shift of mutant channel in response to 25 μM diC_8 $PI(4,5)P_2$. The shift with diC_8 $PI(4,5)P_2$ in the presence of cAMP is less than the shift with diC_8 $PI(4,5)P_2$ alone (PIP_2) (*, $P < 0.01$, *t* test). Error bars show SEM. Number of experiments shown in each bar. (B) Interaction of effects of cAMP and diC_8 $PI(4,5)P_2$ on time constants (τ) of HCN2 activation (left axis) and deactivation (right axis). Squares, data obtained in absence of PIP_2 and cAMP (solid line, $n = 14$); circles, data obtained in the presence of 25 μM diC_8 $PI(4,5)P_2$ (dashed line, $n = 10$); triangles, data obtained in presence of 10 μM cAMP (dotted line, $n = 4$); inverted triangles, data obtained in combined presence of 10 μM cAMP plus 25 μM diC_8 $PI(4,5)P_2$ (dash dotted line, $n = 4$). The difference between the time constant of activation at −105 mV in the presence of cAMP (1.49 ± 0.20 s) versus that in the presence of cAMP and PIP_2 (0.664 ± 0.056 s) was statistically significant (*, $P < 0.02$, *t* test). The difference between the time constant of activation at −95 mV in the presence of cAMP (5.66 ± 0.48 s) and in the presence of cAMP and PIP_2 (2.18 ± 0.33 s) was also statistically significant (**, $P < 0.001$, *t* test).

current deactivation (Fig. 4 B). As discussed above, in the absence of cAMP, diC_8 $PI(4,5)P_2$ caused a significant slowing of tail current deactivation at −40 mV. cAMP also slowed the tail current kinetics at −40 mV and, importantly, these effects were occluded by diC_8 $PI(4,5)P_2$. Thus, the rate of channel deactivation at −40 mV in the combined presence of cAMP and diC_8 $PI(4,5)P_2$ was similar to that observed in the presence of diC_8 $PI(4,5)P_2$ alone, indicating that the two modulatory agents share certain common mechanisms of action.

We observed a more complex interaction between cAMP and diC_8 $PI(4,5)P_2$ on activation kinetics. As previously described, cAMP application markedly accelerated HCN2 activation kinetics over a wide range of hyperpolarized voltages (Wainger et al., 2001; Fig. 4 B). In contrast, as mentioned above, diC_8 $PI(4,5)P_2$ caused a modest slowing of activation kinetics at very negative voltages (−135 mV), with no significant effect on activation kinetics at more positive potentials (see Fig. 2 B). However, when we applied diC_8 $PI(4,5)P_2$ in the presence of cAMP, the lipid now produced a significant speeding in the rate of channel activation ($P < 0.02$ at −105 mV and $P < 0.001$ at −95 mV; *t* test; Fig. 4 B) at less hyperpolarized voltages. These results reinforce the notion that cAMP and PIP_2 alter channel gating through both shared and unique mechanisms.

cAMP and diC_8 $PI(4,5)P_2$ Shift HCN2 Activation through Distinct Transduction Mechanisms

To further investigate the relation between the effects of diC_8 $PI(4,5)P_2$ and cAMP on HCN2 gating, we next examined a mutant HCN2 channel in which a tripeptide sequence—Q450, E451, K452—in the first α helix of the C-linker region (which couples the transmembrane domain to the cyclic nucleotide binding domain) was replaced with a tripeptide sequence, FPN, present at the corresponding region of a cyclic nucleotide-gated channel β subunit. This mutation was previously found to reverse the normal polarity of cyclic nucleotide gating of HCN2 so that cAMP binding shifts voltage-dependent opening of the mutant in the hyperpolarizing direction (Zhou et al., 2004). Thus, if $PI(4,5)P_2$ acts through a similar molecular mechanism as does cAMP, FPN mutant channels should show a hyperpolarizing response to phospholipid. In fact, we found that diC_8 $PI(4,5)P_2$ facilitated the opening of HCN2/FPN channels, producing a normal-sized +13.9 ± 1.6-mV shift ($n = 4$; Fig. 4 A). Thus, $PI(4,5)P_2$ must regulate HCN2 gating through a transduction mechanism distinct from that used by cAMP, although the effects of the two modulators clearly interact at several different levels.

Rundown of HCN2 Due to Dephosphorylation of Endogenous PIP_2

The above results clearly show that HCN2 is modulated by exogenous $PI(4,5)P_2$. We next asked whether HCN2 is also modulated by endogenous $PI(4,5)P_2$ and whether the rundown upon patch excision may be due to hydrolysis of endogenous $PI(4,5)P_2$ by membrane-bound lipid

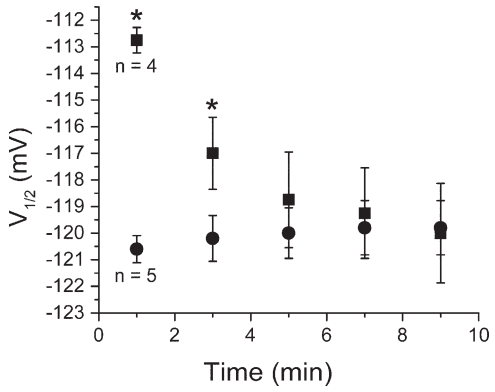

Figure 5. Phosphatase inhibitors delay the rundown in $V_{1/2}$. $V_{1/2}$ values were assessed after inside-out patches were excised into normal bath solution (circles) or FV bath solution to inhibit phosphatase activity (squares). The differences in respective $V_{1/2}$ values measured 1 and 3 min after patch excision were statistically significant (*, $P < 0.05$, *t* test).

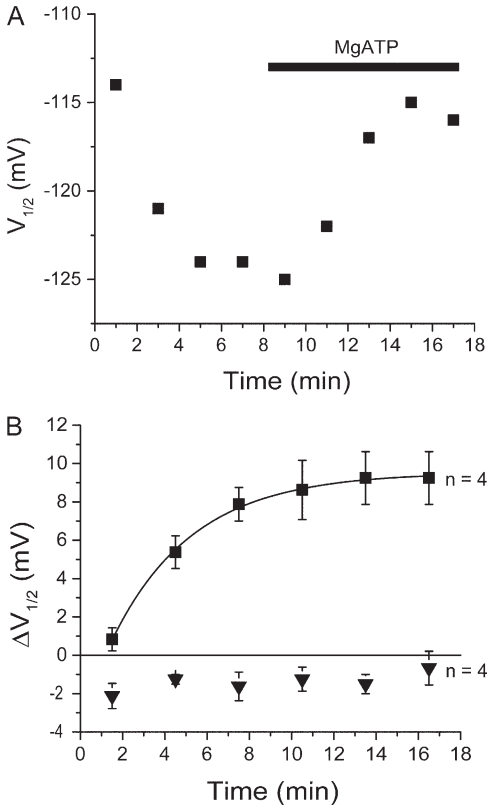

Figure 6. Application of MgATP to inside-out patches shifts HCN2 activation to more positive voltages. (A) Time course of $V_{1/2}$ of HCN2 in a single inside-out patch experiment showing rundown and response to MgATP. Experiment performed in FV solution to inhibit endogenous phosphatase activity. (B) Time course of average $V_{1/2}$ shift after bath application of MgATP in absence (squares) or presence (inverted triangles) of 15 μM wortmannin to block PI kinases. For data in response to MgATP alone, the single exponential fit yielded values for the steady-state shift in $V_{1/2}$ of +9.5 mV and a $t_{1/2}$ of 3.8 min.

phosphatases, as observed for other channels (Logothetis and Zhang, 1999; Wu et al., 2002).

As a first test of this hypothesis, we examined rundown in the presence of the nonspecific phosphatase inhibitors fluoride (Fl^-) and orthovanadate (VO_4^{3-}), which should block or delay any rundown due to lipid dephosphorylation. Patches containing HCN2 were excised into normal bath solution or bath solution supplemented with 0.1 mM Fl^- and 0.2 mM VO_4^{3-} (FV bath solution; Fig. 5). 1 min after patch excision into normal bath solution, the $V_{1/2}$ of HCN2 was -120.6 ± 0.5 mV ($n = 5$). The $V_{1/2}$ then remained relatively constant over the next 10 min, indicating that rundown was normally complete within 1 min. However, 1 min after patch excision in FV solution, the $V_{1/2}$ was significantly more depolarized than in normal solution (-112.8 ± 0.5 mV; $n = 4$; $P < 0.00001$; *t* test). The $V_{1/2}$ then gradually shifted to more hyperpolarized potentials over the next 5–10 min. The $V_{1/2}$ for HCN2 in patches excised in FV solution remained significantly positive to the $V_{1/2}$ observed in normal bath solution up to 3 min after patch excision ($P < 0.04$; *t* test). However, by 5 min after patch excision, the difference was no longer statistically significant. Thus the phosphatase inhibitors fluoride and orthovanadate delayed but did not prevent HCN2 channel rundown, suggesting that phosphatase activity in the excised patch may contribute to HCN2 channel rundown.

Previous studies suggest that lipid kinases remain associated with the membrane in cell-free patches (e.g., Huang et al., 1998; Rohacs et al., 2002). Thus, as a further test of the hypothesis that endogenous $PI(4,5)P_2$ contributes to the regulation of HCN2, we next examined whether the effects of rundown on the $V_{1/2}$ could be reversed through lipid kinase-mediated phosphorylation. After allowing channel rundown in FV bath solution to reach completion, patches were perfused with FV bath solution plus 2 mM MgATP to promote phosphorylation. Under these conditions, the HCN2 activation curve gradually shifted to more depolarized potentials (Fig. 6 A), reaching an average maximal shift of $+9.3 \pm 1.4$ mV ($n = 4$) with a $t_{1/2}$ of 3.8 min (Fig. 6 B).

This effect of MgATP was due to lipid phosphorylation, as opposed to protein phosphorylation, since we found that the depolarizing shift with MgATP was blocked by the lipid kinase inhibitor wortmannin (15 μM). In the presence of wortmannin, MgATP produced only a -1.0 ± 1.0 mV ($n = 4$) shift in the $V_{1/2}$. In the presence of DMSO alone (the vehicle for wortmannin), addition of MgATP shifted the $V_{1/2}$ by $+7.8 \pm 1.1$ mV ($n = 4$) (Fig. 6 B and Fig. 8), which was not significantly different from the MgATP-induced shift in the absence of DMSO (+9.3 mV; $P > 0.5$; ANOVA). The shifts with MgATP in the absence or presence of DMSO were both significantly greater than the shift in the presence of wortmannin ($P < 0.05$; ANOVA).

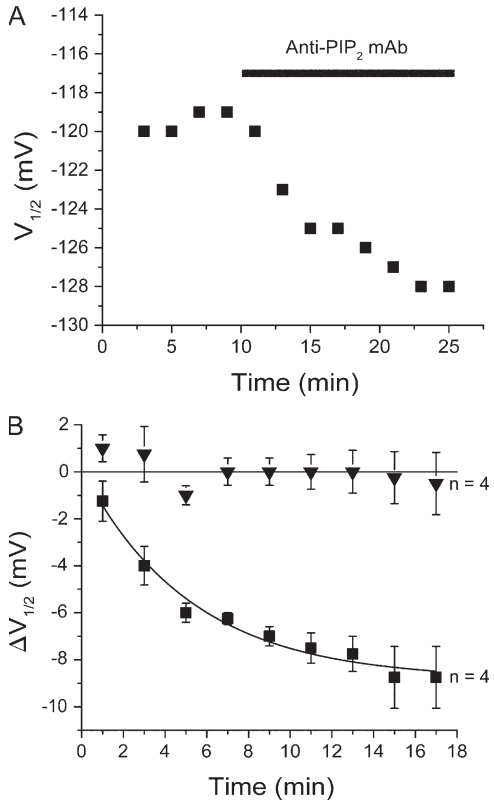

Figure 7. Reducing endogenous $PI(4,5)P_2$ levels shifts HCN2 activation to more negative voltages. (A) Time course of $V_{1/2}$ in a single inside-out patch experiment in response to bath application of 30.3 μg/ml of anti-$PI(4,5)P_2$ antibody. (B) Time course of average $V_{1/2}$ shifts after bath application of anti-$PI(4,5)P_2$ antibody (squares) or heat-inactivated antibody (inverted triangles).

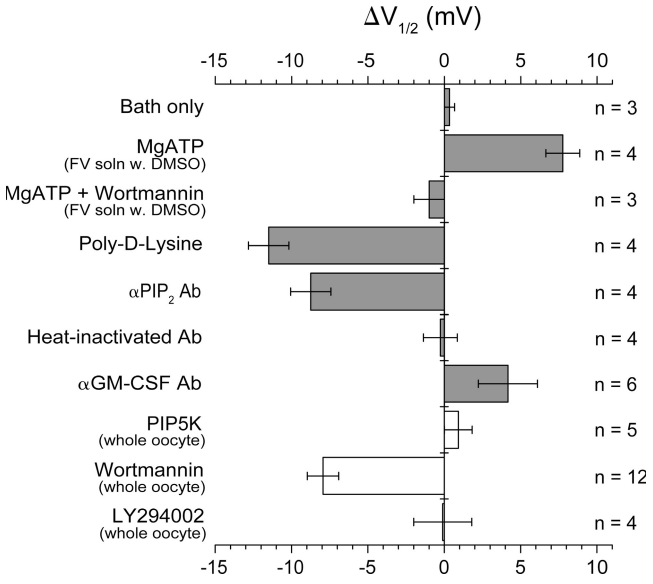

Figure 8. Summary of effects of altering $PI(4,5)P_2$ levels on HCN2 gating. Average shifts in $V_{1/2}$ shown in response to various agents using either inside-out patches (gray bars) or whole oocytes (open bars). From top to bottom: bath only (no treatment); 2 mM MgATP (in FV solution, 0.05% DMSO); 2 mM MgATP plus 15 μM wortmannin (in FV solution, 0.05% DMSO); 25 μg/ml poly-D-lysine; 30.3 μg/ml anti-$PI(4,5)P_2$ antibody (αPIP_2 Ab); 30.3 μg/ml heat-inactivated anti-$PI(4,5)P_2$ antibody; 30.3 μg/ml anti-granulocyte macrophage colony stimulating factor antibody (αGM-CSF Ab); $V_{1/2}$ of HCN2 coexpressed with PI(4)P 5-kinase minus $V_{1/2}$ of HCN2 expressed alone (PIP5K); $V_{1/2}$ of HCN2 after 30–40-min preincubation in 15 μM wortmannin and 0.05% DMSO minus $V_{1/2}$ after preincubation in 0.05% DMSO alone (Wortmannin); $V_{1/2}$ after 2-h preincubation in 20 μM LY294002 and 0.1% DMSO minus $V_{1/2}$ after preincubation in 0.1% DMSO alone (LY294002). Error bars show SEM. Number of experiments shown next to each bar (n).

Next we examined the effect of reducing endogenous $PI(4,5)P_2$ levels by applying to inside-out patches an anti-$PI(4,5)P_2$ antibody (Huang et al., 1998). After rundown had reached completion in normal solution, application of 30.3 μg/ml anti-$PI(4,5)P_2$ antibody caused an additional 8.8 ± 1.3 mV hyperpolarizing shift with a time course characterized by a $t_{1/2}$ of 3.6 min (Fig. 7 B). Control experiments performed with a heat-inactivated anti-$PI(4,5)P_2$ antibody or an unrelated antibody failed to produce a significant hyperpolarizing shift (Fig. 8). A further test of the role of endogenous $PI(4,5)P_2$ came from experiments in which we applied to inside-out patches polylysine, a polycation that reduces the effective negative charge associated with lipid headgroups (Rohacs et al., 2002). Polylysine (25 μg/ml) caused an additional 11.5 ± 1.3- mV hyperpolarizing shift in the HCN2 activation curve (Fig. 8), similar to the effects of the anti-$PI(4,5)P_2$ antibody, consistent with a regulatory function of endogenous phospholipid.

In addition to manipulating $PI(4,5)P_2$ levels in inside-out patches, we also examined the effects of reducing $PI(4,5)P_2$ levels in the plasma membrane of intact oocytes. Oocytes were incubated in 15 μM wortmannin for 30–40 min to block the final step in the biosynthetic pathway for $PI(4,5)P_2$ (Doughman et al., 2003). As a control, other oocytes were incubated in 0.05% DMSO alone. Subsequently, the $V_{1/2}$ values for HCN2 in the intact oocytes were assessed under these two conditions by two-microelectrode voltage clamp. Incubation in wortmannin caused a significant hyperpolarizing shift in the $V_{1/2}$ of −7.9 ± 1.0 mV relative to the control values ($n = 12$ pair). As this concentration of wortmannin inhibits both PI-3 kinase and PI-4 kinase, we tested the effects of LY294002, a more specific inhibitor of PI-3 kinase (Vlahos et al., 1994; Browaeys-Poly et al., 2000; Song and Ashcroft, 2001). There was no significant effect on the $V_{1/2}$ when 20 μM LY294002 was applied to intact oocytes (−0.1 ± 1.9 mV shift relative to DMSO control), indicating a role for PI-4 kinase. Thus, the inhibitory action of wortmannin most likely indicates a role for basal levels of endogenous $PI(4,5)P_2$ in regulating HCN2 gating in the intact oocyte (Fig. 8).

Finally, we attempted to elevate levels of $PI(4,5)P_2$ in intact oocytes by overexpressing PIP5K (Winks et al., 2005).

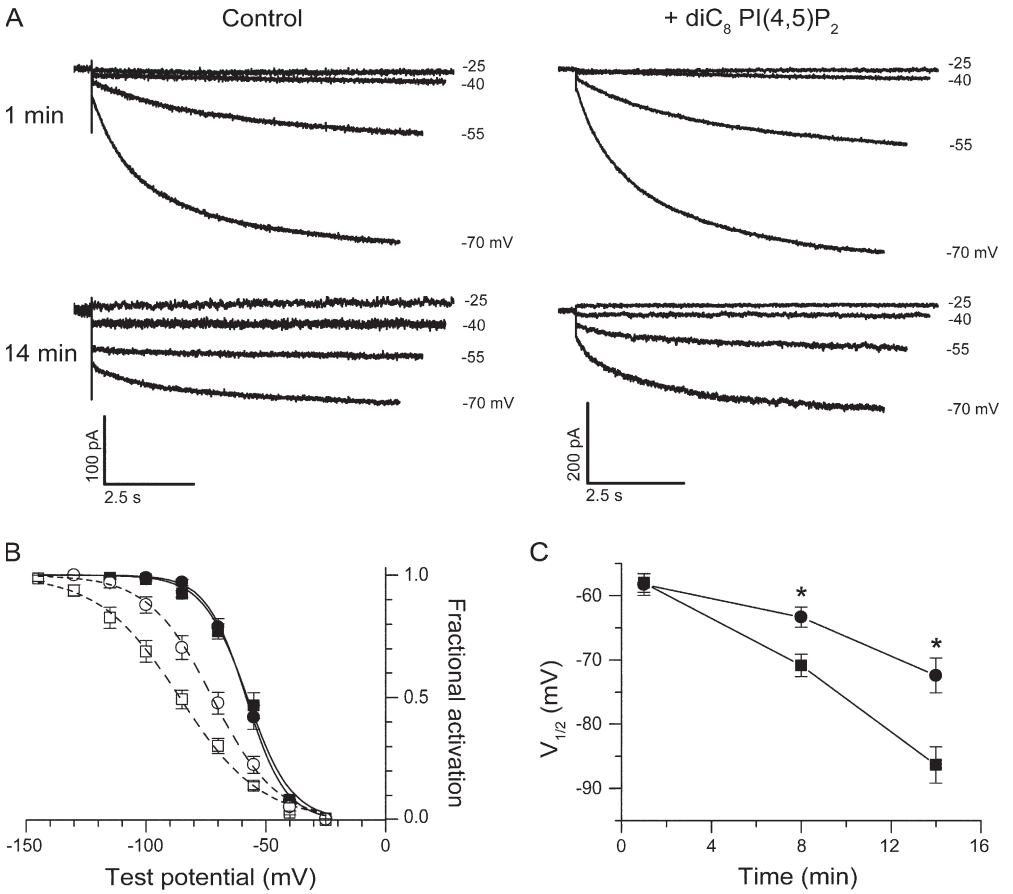

Figure 9. Effect of diC_8 $PI(4,5)P_2$ on the rundown of the voltage dependence of activation for HCN currents in sinoatrial node cells. (A) Representative whole-cell currents evoked by stepping the membrane from a holding potential of −35 mV to voltages ranging from −25 to −70 mV in 15-mV increments. The recordings were acquired 1 min (top) and 14 min (bottom) after membrane rupture in the absence (left) and in the presence (right) of 200 μM diC_8 $PI(4,5)P_2$ in the pipette solution. Hyperpolarizing test voltages indicated at right. (B) Mean tail current activation curves at 1 min (filled symbols) and 14 min (open symbols) in the absence (squares) and in the presence of 200 μM diC_8 $PI(4,5)P_2$ (circles). The curves show best fits of the Boltzmann equation. Mean values of parameters from Boltzmann fits of individual activation curves obtained 1 min after patch rupture in absence and presence of diC_8 $PI(4,5)P_2$ were, respectively, $V_{1/2} = -58.0 \pm 1.5$ mV ($n = 8$) and -58.3 ± 1.7 mV ($n = 8$, $P > 0.05$); $s = 8.5 \pm 0.7$ mV and 7.8 ± 0.2 mV ($P > 0.05$). Mean parameters from Boltzmann fits obtained after 14 min of whole-cell recording in absence and presence of diC_8 $PI(4,5)P_2$ were, respectively, $V_{1/2} = -86.4 \pm 2.8$ mV ($n = 6$) and -72.4 ± 2.7 mV ($n = 6$, $P < 0.05$); $s = 16.8 \pm 1.3$ mV and 12.9 ± 0.7 mV ($P < 0.05$). (C) Time course of rundown in $V_{1/2}$ during whole cell recordings in the absence (squares) and in the presence (circles) of 200 μM diC_8 $PI(4,5)P_2$. The two curves differ significantly at times indicated by asterisks. Values of $V_{1/2}$ for 1- and 14-min points from B. For 8-min points, mean activation parameters in absence and presence of diC_8 $PI(4,5)P_2$ were, respectively, $V_{1/2} = -70.9 \pm 1.7$ mV ($n = 8$) and -63.4 ± 1.6 mV ($n = 8$, $P < 0.05$) and $s = 14.1 \pm 0.3$ mV and 10.9 ± 0.6 mV ($P < 0.05$). Data for B and C obtained from three animals. There was no difference in mean capacitance between the two groups (not depicted).

However, paired two-microelectrode voltage-clamp recordings showed no effect of PIP5K overexpression (0.9 ± 0.9 mV difference), perhaps indicating that endogenous PIP5K is not rate limiting for $PI(4,5)P_2$ production in the oocytes (Fig. 8).

Regulation of Native HCN Currents in Sinoatrial Node Cells by DiC_8 $PI(4,5)P_2$

Are native HCN currents in rabbit cardiac sinoatrial cells also regulated by exogenous $PI(4,5)P_2$? To address this question, we evaluated the effect of intracellular dialysis with diC_8 $PI(4,5)P_2$ on the normal rundown of sinoatrial HCN currents during whole cell recording. The voltage dependence of activation was assayed by a two-step voltage protocol (see Materials and methods), in the absence or in the presence of diC_8 $PI(4,5)P_2$ (200 μM) in the patch pipette solution (Fig. 9 A). Activation curves determined in the presence or absence of diC_8 $PI(4,5)P_2$ were identical when measured 1 min after the start of whole-cell recording, with $V_{1/2}$ values of −58 mV (Fig. 9 B). However, after 14 min of whole cell recording, the two activation curves were clearly different. In the absence of diC_8 $PI(4,5)P_2$, the $V_{1/2}$ shifted to −86 mV, reflecting rundown. In contrast, with diC_8 $PI(4,5)P_2$ in the pipette solution, the $V_{1/2}$ only shifted to −72 mV (Fig. 9 B). A plot of $V_{1/2}$ versus duration of whole-cell recording revealed the progressive hyperpolarizing shift in the HCN activation curve, in both the absence and presence of diC_8 $PI(4,5)P_2$ (Fig. 9 C). However, diC_8 $PI(4,5)P_2$ clearly delayed the hyperpolarizing shift, with statistically significant positive shifts observed for the 8- and 14-min time points ($P < 0.05$).

DISCUSSION

The present study provides strong support for the view that $PI(4,5)P_2$ regulates both recombinant HCN2 and native cardiac HCN channels and that its degradation

after patch excision contributes to channel rundown. Thus, application of exogenous $PI(4,5)P_2$ reversed rundown, whereas sequestration of $PI(4,5)P_2$ enhanced rundown. Moreover, rundown was slowed by inhibition of phosphatases and partly reversed when endogenous lipid kinases were supplied with MgATP. Finally, manipulation of $PI(4,5)P_2$ levels in intact oocytes also modulated HCN2 gating.

Comparison of Effects of PIP_2 on HCN2 with Other Channels

HCN2 joins a growing list of channels regulated by $PI(4,5)P_2$ (Suh and Hille, 2005). For some channels, such as TRPV1 (Chuang et al., 2001) and mammalian rod cyclic nucleotide-gated channels (Womack et al., 2000), $PI(4,5)P_2$ inhibits channel activity. However, for the majority of channels regulated by $PI(4,5)P_2$, including HCN2, $PI(4,5)P_2$ is permissive for channel activity (Hilgemann et al., 2001). Previous studies that investigated the role of $PI(4,5)P_2$ in channel regulation usually characterized changes in channel function in response to depletion or addition of phosphoinositides to intact membranes. Such studies with the family of inward rectifying K^+ channels (K_{ir}) have demonstrated a spectrum of apparent $PI(4,5)P_2$ affinities among different channels. Our experiments indicate that HCN2 falls into the K_{ATP} class of channels with relative low specificity for phosphoinositides.

Although HCN2 showed a relatively low selectivity among the polyphosphoinositides, the channel may have a relatively high affinity for $PI(4,5)P_2$. Channels that tightly bind $PI(4,5)P_2$ show a very slow response to application of the anti-$PI(4,5)P_2$ antibody, whereas channels that weakly bind $PI(4,5)P_2$ are rapidly inhibited by the antibody. For example, the high-affinity IRK1 channel is inhibited by anti-$PI(4,5)P_2$ antibody with a half-time of $\sim$90 s, whereas the low-affinity GIRK1/4 and GIRK2 channels show half-maximal block in $<$10 s (Huang et al., 1998). Despite our having used slightly higher concentrations of antibody than used in the K_{ir} studies, we found that HCN2 required $>$200 s for half-maximal inhibition with the anti-$PI(4,5)P_2$ antibody, suggesting that HCN2 has a high affinity for $PI(4,5)P_2$ (although we cannot rule out the possibility that the slow time course of inhibition is due to a particularly slow access of antibody to the inside membrane of the patch in our experiments). A high affinity of HCN2 for $PI(4,5)P_2$ is consistent with the idea that this channel constitutively binds $PI(4,5)P_2$ and that hydrolysis of this phospholipid underlies the ubiquitous rundown of HCN currents.

Interactions of cAMP and PIP_2: Mechanistic Implications

Our results, unfortunately, do not provide a definitive mechanism for how $PI(4,5)P_2$ regulates HCN2 gating. However, a comparison with the modulatory effects of cAMP provides some interesting clues. The binding of cAMP to its C-terminal cyclic nucleotide binding domain is thought to facilitate HCN channel opening by relieving an inhibitory action of the C terminus on gating (Wainger et al., 2001). Moreover, the effect of cAMP binding to the CNBD is transduced into changes in channel opening through the intervening C-linker region (Chen et al., 2001). We find that a C-linker mutation that reverses the polarity of cAMP action on voltage gating (Zhou et al., 2004) causes no change in $PI(4,5)P_2$ action, indicating that phospholipid must act through a distinct mechanism from cyclic nucleotide. However, our finding that the effects of cAMP and $PI(4,5)P_2$ are not completely additive suggests that the actions of these modulators may converge on some final mechanistic step of gating, such as the opening of the channel gate at the inner surface of the membrane (Rothberg et al., 2003).

Potential Physiological Implications of Modulation by PIP_2

Our study clearly demonstrates that changes in membrane $PI(4,5)P_2$ concentration can affect the gating of recombinant HCN2, with higher levels of $PI(4,5)P_2$ shifting gating to more positive potentials. In addition, we have shown in cells from rabbit sinoatrial node that diC_8 $PI(4,5)P_2$ also delays the onset of native channel rundown in whole cell recordings. These findings suggest that native HCN channels are regulated by $PI(4,5)P_2$ and that the presence of this lipid is required to maintain the relatively depolarized range of activation of HCN channels that is required for their opening at physiologically relevant voltages. Moreover, given that rabbit sinoatrial node cells express primarily HCN4 and HCN1 (Shi et al., 1999), our results further indicate that $PI(4,5)P_2$ is a general modulator of HCN channel function, and does not only target HCN2.

One important remaining question is whether HCN channel function is dynamically regulated in neurons or cardiac myocytes during signal transduction cascades that alter membrane levels of $PI(4,5)P_2$. Receptor-mediated activation of phospholipase C results in a decrease in membrane concentration of $PI(4,5)P_2$ that alters the activity of a number of channels, including GIRK1/4 and KCNQ2/3 (Rohacs et al., 1999; Kobrinsky et al., 2000; Wu et al., 2002; Zhang et al., 2003; Cho et al., 2005). In sinoatrial node cells, a hyperpolarizing shift in HCN channel activation due to reduced levels of $PI(4,5)P_2$ would slow heart rate, similar to the action of nanomolar concentrations of acetylcholine, which cause a hyperpolarizing shift in pacemaker current without affecting other nodal currents (DiFrancesco et al., 1989). However, such regulation is most effective for channels with a relatively low affinity for $PI(4,5)P_2$, which may or may not hold for HCN channels. In addition to acute regulation by receptor activation, basal levels of $PI(4,5)P_2$ may also change during development, times

of stress, or in disease states (Suchy et al., 1995; Soares et al., 1997; Pasquare et al., 2004; Suh and Hille, 2005); these changes could lead to more tonic changes in HCN channel function. Lastly, $PI(4,5)P_2$ levels vary among the different membrane compartments of a cell. Thus, a stimulatory effect of $PI(4,5)P_2$ may allow the cell to restrict channel activity as channels are transported from their site of synthesis in the endoplasmic reticulum to final destinations with more permissive phosphoinositide concentrations (Hilgemann et al., 2001; Suh and Hille, 2005). Further studies will be required to determine the physiological importance of the regulation of HCN channels by $PI(4,5)P_2$.

We thank Gareth Tibbs and Keri Fogle for helpful discussions and sharing unpublished data. We thank John Riley for help with the *Xenopus* oocyte injections.

This work was partially supported by grants NS-36658 (S.A. Siegelbaum) and HL-28958 (R.B. Robinson) from the National Institutes of Health, and the Howard Hughes Medical Institute (S.A. Siegelbaum).

Olaf S. Andersen served as editor.

Submitted: 10 August 2006
Accepted: 12 October 2006

REFERENCES

Arinsburg, S.S., I.S. Cohen, and H.G. Yu. 2006. Constitutively active Src tyrosine kinase changes gating of HCN4 channels through direct binding to the channel proteins. *J. Cardiovasc. Pharmacol.* 47:578–586.

Bois, P., B. Renaudon, M. Baruscotti, J. Lenfant, and D. DiFrancesco. 1997. Activation of f-channels by cAMP analogues in macropatches from rabbit sino-atrial node myocytes. *J. Physiol.* 501(Pt 3): 565–571.

Browaeys-Poly, E., K. Cailliau, and J.P. Vilain. 2000. Signal transduction pathways triggered by fibroblast growth factor receptor 1 expressed in *Xenopus laevis* oocytes after fibroblast growth factor 1 addition. Role of Grb2, phosphatidylinositol 3-kinase, Src tyrosine kinase, and phospholipase Cγ. *Eur. J. Biochem.* 267:6256–6263.

Cerbai, E., R. Pino, F. Porciatti, G. Sani, M. Toscano, M. Maccherini, G. Giunti, and A. Mugelli. 1997. Characterization of the hyperpolarization-activated current, I(f), in ventricular myocytes from human failing heart. *Circulation.* 95:568–571.

Chen, S., J. Wang, and S.A. Siegelbaum. 2001. Properties of hyperpolarization-activated pacemaker current defined by coassembly of HCN1 and HCN2 subunits and basal modulation by cyclic nucleotide. *J. Gen. Physiol.* 117:491–504.

Cho, H., D. Lee, S.H. Lee, and W.K. Ho. 2005. Receptor-induced depletion of phosphatidylinositol 4,5-bisphosphate inhibits inwardly rectifying K^+ channels in a receptor-specific manner. *Proc. Natl. Acad. Sci. USA.* 102:4643–4648.

Chuang, H.H., E.D. Prescott, H. Kong, S. Shields, S.E. Jordt, A.I. Basbaum, M.V. Chao, and D. Julius. 2001. Bradykinin and nerve growth factor release the capsaicin receptor from PtdIns(4,5)P2-mediated inhibition. *Nature.* 411:957–962.

DiFrancesco, D. 2006. Funny channels in the control of cardiac rhythm and mode of action of selective blockers. *Pharmacol. Res.* 53:399–406.

DiFrancesco, D., P. Ducouret, and R.B. Robinson. 1989. Muscarinic modulation of cardiac rate at low acetylcholine concentrations. *Science.* 243:669–671.

DiFrancesco, D., A. Ferroni, M. Mazzanti, and C. Tromba. 1986. Properties of the hyperpolarizing-activated current (i_f) in cells isolated from the rabbit sino-atrial node. *J. Physiol.* 377:61–88.

DiFrancesco, D., and M. Mangoni. 1994. Modulation of single hyperpolarization-activated channels (i(f)) by cAMP in the rabbit sino-atrial node. *J. Physiol.* 474:473–482.

DiFrancesco, D., and P. Tortora. 1991. Direct activation of cardiac pacemaker channels by intracellular cyclic AMP. *Nature.* 351:145–147.

Doughman, R.L., A.J. Firestone, and R.A. Anderson. 2003. Phosphatidylinositol phosphate kinases put PI4,5P(2) in its place. *J. Membr. Biol.* 194:77–89.

Goulding, E.H., J. Ngai, R.H. Kramer, S. Colicos, R. Axel, S.A. Siegelbaum, and A. Chess. 1992. Molecular cloning and single-channel properties of the cyclic nucleotide-gated channel from catfish olfactory neurons. *Neuron.* 8:45–58.

Hilgemann, D.W., S. Feng, and C. Nasuhoglu. 2001. The complex and intriguing lives of PIP2 with ion channels and transporters. *Sci. STKE.* 2001:RE19.

Huang, C.L., S. Feng, and D.W. Hilgemann. 1998. Direct activation of inward rectifier potassium channels by PIP2 and its stabilization by Gβγ. *Nature.* 391:803–806.

Kobrinsky, E., T. Mirshahi, H. Zhang, T. Jin, and D.E. Logothetis. 2000. Receptor-mediated hydrolysis of plasma membrane messenger PIP2 leads to K^+-current desensitization. *Nat. Cell Biol.* 2:507–514.

Logothetis, D.E., and H. Zhang. 1999. Gating of G protein-sensitive inwardly rectifying K^+ channels through phosphatidylinositol 4,5-bisphosphate. *J. Physiol.* 520(Pt. 3):630.

McLaughlin, S., J. Wang, A. Gambhir, and D. Murray. 2002. PIP(2) and proteins: interactions, organization, and information flow. *Annu. Rev. Biophys. Biomol. Struct.* 31:151–175.

Pasquare, S.J., G.A. Salvador, and N.M. Giusto. 2004. Phospholipase D and phosphatidate phosphohydrolase activities in rat cerebellum during aging. *Lipids.* 39:553–560.

Qu, J., A. Barbuti, L. Protas, B. Santoro, I.S. Cohen, and R.B. Robinson. 2001. HCN2 overexpression in newborn and adult ventricular myocytes: distinct effects on gating and excitability. *Circ. Res.* 89:E8–14.

Robinson, R.B., and S.A. Siegelbaum. 2003. Hyperpolarization-activated cation currents: from molecules to physiological function. *Annu. Rev. Physiol.* 65:453–480.

Robinson, R.B., H. Yu, F. Chang, and I.S. Cohen. 1997. Developmental change in the voltage-dependence of the pacemaker current, if, in rat ventricle cells. *Pflugers Arch.* 433:533–535.

Rohacs, T., J. Chen, G.D. Prestwich, and D.E. Logothetis. 1999. Distinct specificities of inwardly rectifying K^+ channels for phosphoinositides. *J. Biol. Chem.* 274:36065–36072.

Rohacs, T., C. Lopes, T. Mirshahi, T. Jin, H. Zhang, and D.E. Logothetis. 2002. Assaying phosphatidylinositol bisphosphate regulation of potassium channels. *Methods Enzymol.* 345:71–92.

Rohacs, T., C.M. Lopes, T. Jin, P.P. Ramdya, Z. Molnar, and D.E. Logothetis. 2003. Specificity of activation by phosphoinositides determines lipid regulation of Kir channels. *Proc. Natl. Acad. Sci. USA.* 100:745–750.

Rothberg, B.S., K.S. Shin, and G. Yellen. 2003. Movements near the gate of a hyperpolarization-activated cation channel. *J. Gen. Physiol.* 122:501–510.

Santoro, B., B.J. Wainger, and S.A. Siegelbaum. 2004. Regulation of HCN channel surface expression by a novel C-terminal protein-protein interaction. *J. Neurosci.* 24:10750–10762.

Shi, W., R. Wymore, H. Yu, J. Wu, R.T. Wymore, Z. Pan, R.B. Robinson, J.E. Dixon, D. McKinnon, and I.S. Cohen. 1999. Distribution and prevalence of hyperpolarization-activated cation channel (HCN) mRNA expression in cardiac tissues. *Circ. Res.* 85:e1–e6.

Soares, J.C., C.S. Dippold, and A.G. Mallinger. 1997. Platelet membrane phosphatidylinositol-4,5-bisphosphate alterations in bipolar disorder–evidence from a single case study. *Psychiatry Res.* 69:197–202.

Song, D.K., and F.M. Ashcroft. 2001. ATP modulation of ATP-sensitive potassium channel ATP sensitivity varies with the type of SUR subunit. *J. Biol. Chem.* 276:7143–7149.

Suchy, S.F., I.M. Olivos-Glander, and R.L. Nussabaum. 1995. Lowe syndrome, a deficiency of phosphatidylinositol 4,5-bisphosphate 5-phosphatase in the Golgi apparatus. *Hum. Mol. Genet.* 4:2245–2250.

Suh, B.C., and B. Hille. 2005. Regulation of ion channels by phosphatidylinositol 4,5-bisphosphate. *Curr. Opin. Neurobiol.* 15: 370–378.

Vlahos, C.J., W.F. Matter, K.Y. Hui, and R.F. Brown. 1994. A specific inhibitor of phosphatidylinositol 3-kinase, 2-(4-morpholinyl)-8-phenyl-4H-1-benzopyran-4-one (LY294002). *J. Biol. Chem.* 269: 5241–5248.

Wainger, B.J., M. DeGennaro, B. Santoro, S.A. Siegelbaum, and G.R. Tibbs. 2001. Molecular mechanism of cAMP modulation of HCN pacemaker channels. *Nature.* 411:805–810.

Winks, J.S., S. Hughes, A.K. Filippov, L. Tatulian, F.C. Abogadie, D.A. Brown, and S.J. Marsh. 2005. Relationship between membrane phosphatidylinositol-4,5-bisphosphate and receptor-mediated inhibition of native neuronal M channels. *J. Neurosci.* 25:3400–3413.

Womack, K.B., S.E. Gordon, F. He, T.G. Wensel, C.C. Lu, and D.W. Hilgemann. 2000. Do phosphatidylinositides modulate vertebrate phototransduction? *J. Neurosci.* 20:2792–2799.

Wu, L., C.S. Bauer, X.G. Zhen, C. Xie, and J. Yang. 2002. Dual regulation of voltage-gated calcium channels by PtdIns(4,5)P2. *Nature.* 419:947–952.

Yu, H., J. Wu, I. Potapova, R.T. Wymore, B. Holmes, J. Zuckerman, Z. Pan, H. Wang, W. Shi, R.B. Robinson, et al. 2001. MinK-related peptide 1: A β subunit for the HCN ion channel subunit family enhances expression and speeds activation. *Circ. Res.* 88:E84–E87.

Yu, H.G., Z. Lu, Z. Pan, and I.S. Cohen. 2004. Tyrosine kinase inhibition differentially regulates heterologously expressed HCN channels. *Pflugers Arch.* 447:392–400.

Zhang, H., L.C. Craciun, T. Mirshahi, T. Rohacs, C.M. Lopes, T. Jin, and D.E. Logothetis. 2003. PIP(2) activates KCNQ channels, and its hydrolysis underlies receptor-mediated inhibition of M currents. *Neuron.* 37:963–975.

Zhang, H., C. He, X. Yan, T. Mirshahi, and D.E. Logothetis. 1999. Activation of inwardly rectifying K^+ channels by distinct PtdIns(4,5)P2 interactions. *Nat. Cell Biol.* 1:183–188.

Zhou, L., N.B. Olivier, H. Yao, E.C. Young, and S.A. Siegelbaum. 2004. A conserved tripeptide in CNG and HCN channels regulates ligand gating by controlling C-terminal oligomerization. *Neuron.* 44:823–834.

Zhou, Z., and S.L. Lipsius. 1993. Effect of isoprenaline on I_f current in latent pacemaker cells isolated from cat right atrium: ruptured vs. perforated patch whole-cell recording methods. *Pflugers Arch.* 423:442–447.

Zong, X., C. Eckert, H. Yuan, C. Wahl-Schott, H. Abicht, L. Fang, R. Li, P. Mistrik, A. Gerstner, B. Much, et al. 2005. A novel mechanism of modulation of hyperpolarization-activated cyclic nucleotide-gated channels by Src kinase. *J. Biol. Chem.* 280:34224–34232.